Shaikh, Bushra; Garau Burguera, Pere; Al-Tous, Hanan; Juntti, Markku; Khan, Muhammad Bilal; Tirkkonen, Olav

Channel Charting Based Pilot Allocation in MIMO Systems

Published in:
Proceedings of the IEEE International Symposium on Personal, Indoor and Mobile Radio Communications

Accepted/In press: 01/01/2024

Document Version
Peer-reviewed accepted author manuscript, also known as Final accepted manuscript or Post-print

Please cite the original version:
Shaikh, B., Garau Burguera, P., Al-Tous, H., Juntti, M., Khan, M. B., & Tirkkonen, O. (in press). Channel Charting Based Pilot Allocation in MIMO Systems. In *Proceedings of the IEEE International Symposium on Personal, Indoor and Mobile Radio Communications* IEEE.

Channel Charting Based Pilot Allocation in MIMO Systems

Bushra Shaikh[1,2], Pere Garau Burguera[1], Hanan Al-Tous[1], Markku Juntti[3],
Bilal Muhammad Khan[2], and Olav Tirkkonen[1]

[1]Department of Information and Communications Engineering, Aalto University, Finland
[2]Department of Electronics and Power Engineering, National University of Sciences and Technology, Pakistan
[3]Centre for Wireless Communications, University of Oulu, Finland
Email: {bushra.shaikh, pere.garauburguera, hanan.al-tous, olav.tirkkonen}@aalto.fi,
markku.juntti@oulu.fi, bmkhan@pnec.nust.edu.pk

***Abstract*—We consider uplink pilot allocation based on multi-point channel charting (CC) to mitigate pilot contamination in a multi-cell network with spatially correlated MIMO channels. The channel chart is created in an offline phase with full information, i.e. user channel covariance matrices are estimated at multiple base stations (BSs). In the online phase, we assume that only partial information about a user's channel covariance is known, i.e., it is available only at the serving BS. A machine learning framework is developed to predict the CC locations in the online phase. Pilots are allocated to active users in the online phase based on weighted graph colouring. CC locations are used as proxies of user locations; similarity weights between users are constructed from CC distances. Simulation results show that the CC based approach with partial information in the online phase outperforms a solution based on full angle-of-arrival information, and performs closely to an algorithm with full covariance information. We also consider a partial information machine learning framework to predict the channel covariance matrices at other BSs, which slightly outperforms CC based approach, with the price of a larger communication overhead and computational complexity.**

***Index Terms*—Multi-cell systems, pilot allocation, channel charting, channel covariance.**

I. Introduction

Massive multiple-input multiple-output (mMIMO) communications provides spatial multiplexing gain, enabling uplink reception of transmissions from multiple user equipment (UE) if accurate channel state information (CSI) is available at the base station (BS) [1]. For channel estimation, UEs send uplink training signals (pilots) to the BSs. As the number of orthogonal pilot sequences is limited, there is pilot contamination which degrades the performance. To reduce its effect, many intelligent pilot allocation schemes have been proposed in the literature [2]–[7]. In these works, the second order channel statistics of UEs such as large scale fading coefficients, channel covariance matrices, or UE and BS location information are utilized. In covariance-aware pilot allocation [3], [8], orthogonal pilots are assigned when two covariance matrices are mutually uncorrelated. Location-aware pilot allocation schemes such as in [4], [6], [7] exploit angle-of-arrival (AoA) information of UEs and assign orthogonal pilots to UEs having overlapping AoA ranges. Pilots are allocated either by optimizing a network utility function or by considering a weighted graph coloring (WGC) problem on an interference graph.

Pilot allocation in mMIMO systems can be based on either a centralized or a distributed interference graph. In the centralized case, all BSs together create one interference graph and then apply a pilot allocation algorithm [5]. This solution is based on an assumption that information such as channel covariance or AoA is available at all BSs. In the distributed case, each BS constructs its own interference graph and then applies a pilot allocation algorithm [7]. The distributed approach can be improved by considering a coordination framework where each BS updates the pilot allocation in its cell while the pilots in other cells are kept the same.

In [9], *channel charting* (CC) is proposed as a method to create pseudo-positions of UEs based on slowly varying channel characteristics. CC exploits the spatial information existing in the CSI to create an unsupervised low-dimensional map of UEs, in which the relative positions of UEs are preserved. CC can be utilized in many radio resource management (RRM) tasks, including handover and signal-to-noise-ratio (SNR) prediction and pilot allocation [10]–[12]. In [11], CC was used to mitigate pilot contamination and to improve channel estimation accuracy in a single-cell mMIMO system. In [12], the pilot allocation algorithm is extended to multi-cell mMIMO systems, assuming full knowledge of UE channel covariance matrices.

In this paper we provide an uplink mMIMO pilot allocation framework where CC locations are used as a proxy of physical locations of UEs. In an offline phase, a multipoint CC is constructed based on full channel covarriance information of sample UEs at multiple BSs. In an online phase, pilot allocation is performed for a population of active users based on channel covariance information only at the serving BS.

The main contributions of this paper are: *i)* We improve the CC on the offline phase by merging the information of all sectors served by a BS, assuming phase coherence between sectors, before merging the non-phase-coherent points-of-view of all BSs. *ii)* We consider limited knowledge about channel covariance matrices in the online phase, and develop a method

for placing out-of-sample (OoS) UEs onto the multi-point CC. *iii)* We use the CC distances of OoS UEs to create a weighted graph on which a greedy pilot allocation algorithm is executed. *iv)* We develop a machine learning approach to predict the covariance matrices at other cells for OoS UEs and use these for weighted graph coloring greedy pilot allocation.

The remainder of this paper is organized as follows: In Section II and III, the system model and channel estimation is presented, respectively. In Section IV, CC is explained. In Section V, pilot allocation methods are discussed. In Section VI, the proposed learning framework is presented. Simulation results are presented and discussed in Section VII. Finally, conclusions are drawn in Section VIII.

II. System Model

We consider a multi-cell mMIMO system, consisting of B BSs, with each BS area split into S sectors, each of which is a logical cell. The total number of sectors (cells) is $C = SB$. Each sector is equipped with an M'-element uniform linear array (ULA). The total number of antennas at each BS is $M = SM'$. The cells/sectors in the network are indexed as

$$c = s + (b-1)S, \text{ for } s = 1, \ldots, S, \ b = 1, \ldots .B.$$

The total number of UEs is K, and the set of UEs served by cell c is denoted by $\mathcal{I}_c$. For simplicity, we assume that each UE has a single omnidirectional antenna, handling more involved UE antenna configurations is left for future work. The channel gain $\mathbf{h}_{c,k} \in \mathbb{C}^{M'}$ of UE k in cell c is

$$\mathbf{h}_{c,k} = \sqrt{L_{b,k}} \sum_{p=1}^{P} \sqrt{A\left(\theta_{c,k}^{(p)}\right)}\, \alpha_{c,k}^{(p)}\, \mathbf{a}_{M'}\left(\theta_{c,k}^{(p)}\right), \qquad (1)$$

where $L_{b,k}$ is the large scale fading coefficient, it represents the path loss $L_{b,k} = \frac{\rho_0}{d_{b,k}^{\nu}}$, with ρ_0 the path loss at the reference distance of 1 m, and ν the path loss exponent, $d_{b,k}$ is the distance between BS b and UE k, and P is the number of multi-path components. The instantaneous channel gain of component p is represented by $\alpha_{c,k}^{(p)} \in \mathbb{C}$. The azimuth angle of arrival from path p is $\theta_{c,k}^{(p)}$, and the array response vector is

$$\mathbf{a}_{M'}(\theta) = \left[1, e^{2j\pi\mu\sin\theta}, \ldots, e^{2j\pi\mu(M'-1)\sin\theta}\right]^{\mathrm{T}},$$

where μ is the element spacing in units of wavelength. The antenna gain for each ULA is modeled as [13]:

$$A(\theta)_{\mathrm{dB}} = G_{\max}(\theta) - \min\left\{12\left(\frac{\theta}{\theta_{3\mathrm{dB}}}\right)^2,\ A_{\max}\right\}, \qquad (2)$$

where θ is the angle, $\theta_{3\mathrm{dB}}$ is the 3 dB beamwidth, $G_{\max}$ is the maximum antenna gain, and $A_{\max}$ is the maximum attenuation. The channel covariance matrix of UE k at cell c is

$$\mathbf{R}_{c,k} = \mathbb{E}\left[\mathbf{h}_{c,k}\mathbf{h}_{c,k}^{\mathrm{H}}\right], \qquad (3)$$

where the expectation is over small-scale fading.

We adopt the one-ring channel model, which assumes that the multi-path components are concentrated around the UE, while the BS is in an elevated position. Each multi-path component impings on the antenna array from a particular angle within a ring close to the UE, making channels spatially correlated with independent gains and phase rotations [14]. The (n,m)th element of the covariance matrix of UE k in cell c can be expressed as:

$$r_{c,k,n,m} = L_{b,k} \int_{-\pi}^{\pi} A(\theta)\ e^{-j2\pi\mu(n-m)\sin(\theta)} f_{\Theta}(\theta)\, d\theta,$$

where $n,\ m = 0, \ldots, M'-1$ are the indices of the ULA elements, $f_{\Theta}(\cdot)$ is the probability density function of the AoA. Note that this covariance matrix is unnormalized, i.e., it captures the large-scale propagation effects. The AoAs for the P paths between UE k and cell c can be modelled as i.i.d. random variables with uniform distribution $\mathcal{U}\left[\theta_{c,k}^{\min},\ \theta_{c,k}^{\max}\right]$, with $\theta_{c,k}^{\min} = \bar{\theta}_{c,k} - \sqrt{3}\sigma_\theta$ and $\theta_{c,k}^{\max} = \bar{\theta}_{c,k} + \sqrt{3}\sigma_\theta$. Here, $\bar{\theta}_{c,k} \in [0, 2\pi]$ is the incident angle at cell c from the signal arriving from UE k, σ_θ is the angular standard deviation. The following approximation can be used for the (n,m)th element of the covariance matrix

$$r_{c,k,n,m} \approx \frac{\beta_{c,k}}{2\sqrt{3}\sigma_\theta} \int_{\theta_{c,k}^{\min}}^{\theta_{c,k}^{\max}} e^{-j2\pi\mu(n-m)\sin(\theta)} d\theta,$$

where $\beta_{c,k} = L_{b,k} A\left(\bar{\theta}_{c,k}\right)$.

III. Channel Estimation

We assume that within one coherence block, the channels are time-invariant and flat fading. In each coherence block, all active UEs transmit known pilot symbols to the BS for channel estimation. During uplink training, K simultaneously active UEs communicate with C cells in the network. The pilot length is $\tau \ll K$ and the pilot codebook is expressed as $\mathbf{\Phi} = [\boldsymbol{\phi}_1, \ldots, \boldsymbol{\phi}_\tau] \in \mathbb{C}^{\tau\times\tau}$, satisfying $\mathbf{\Phi}^{\mathrm{H}}\mathbf{\Phi} = \tau\,\mathbf{I}$. Cell c obtains the CSI for UE k through the pilot signal $\sqrt{\varrho}\boldsymbol{\phi}_{\pi_k}^{\mathrm{T}} \in \mathbb{C}^{1\times\tau}$, where ϱ is the power of each pilot symbol and $\pi_k \in \{1, \ldots, \tau\}$ is the index of the pilot sequence assigned to UE k. The set of interfering UEs (i.e., using the same pilot) to UE k is defined as $\mathcal{J}_k = \{j \mid j \in \mathcal{K}\backslash k,\ \pi_j = \pi_k\}$, where $\mathcal{K}$ is the set of UEs.

The received signal from all pilots at cell c is:

$$\mathbf{Y}_c = \sum_{\rho=1}^{\tau} \mathbf{Y}_{c,\rho} + \mathbf{N},$$

where $\mathbf{N} \in \mathbb{C}^{M'\times\tau}$ is receiver additive white Gaussian noise (AWGN) and the received signal at a cell c using pilot π_k is given by:

$$\mathbf{Y}_{c,\pi_k} = \sqrt{\varrho}\left(\mathbf{h}_{c,k} + \sum_{j\in\mathcal{J}_k} \mathbf{h}_{c,j}\right)\boldsymbol{\phi}_{\pi_k}^{\mathrm{T}}. \qquad (4)$$

The received pilot signal for UE k after correlating $\mathbf{Y}_c$ with $\boldsymbol{\phi}_{\pi_k}$ and normalizing the power is as [3]:

$$\mathbf{y}_{c,k}^{(\mathrm{d})} = \mathbf{h}_{c,k} + \sum_{j\in\mathcal{J}_k} \mathbf{h}_{c,j} + \mathbf{n}, \qquad (5)$$

where $\mathbf{n}$ is the normalized processed noise term, with a per-antenna power of $\frac{\sigma_{\mathrm{n}}^2}{\tau\varrho}$. The received signal contains the sum of channel gains from the desired signal (first term) and pilot interference (second term) caused by both intra- and inter-cell co-pilot UEs. Its covariance matrix is given as:

$$\mathbf{Q}_{c,k} = \mathbf{R}_{c,k} + \sum_{j \in \mathcal{J}_k} \mathbf{R}_{c,j} + \frac{\sigma_{\mathrm{n}}^2}{\tau\varrho}\mathbf{I}, \tag{6}$$

where σ_{n}^2 is the noise power. Under linear minimum mean square error (LMMSE) estimator, the channel of UE k at cell c is given as:

$$\hat{\mathbf{h}}_{c,k} = \mathbf{R}_{c,k}\, \mathbf{Q}_{c,k}^{-1} \mathbf{y}_{c,k}^{(\mathrm{d})}. \tag{7}$$

The covariance matrices are assumed to be estimated in the absence of pilot contamination [3]. The CSI estimation error of UE k is $\tilde{\mathbf{h}}_{c,k} = \mathbf{h}_{c,k} - \hat{\mathbf{h}}_{c,k}$, where $\tilde{\mathbf{h}}_{c,k} \sim \mathrm{CN}(0, \tilde{\mathbf{R}}_{c,k})$, and its covariance matrix is found as [14]:

$$\tilde{\mathbf{R}}_{c,k} = \mathbf{R}_{c,k} - \mathbf{R}_{c,k}\mathbf{Q}_{c,k}^{-1}\mathbf{R}_{c,k}. \tag{8}$$

The normalized mean square error (NMSE) can be used to evaluate the channel estimation performance for all UEs with respect to their cells, and is calculated as:

$$\mathbf{NMSE} = \frac{1}{K}\sum_{c=1}^{C}\sum_{k \in \mathcal{I}_c} \frac{\mathrm{Tr}\left(\tilde{\mathbf{R}}_{c,k}\right)}{\mathrm{Tr}\left(\mathbf{R}_{c,k}\right)}. \tag{9}$$

IV. Channel Charting

CC [9] is an unsupervised framework with the objective of learning a low-dimensional embedding, that locally preserves the geometry of the true locations of the UEs. Channel covariance matrices capture large-scale spatial information that can be used for constructing CSI features. Ideally, a pairwise covariance matrix dissimilarity related to two UEs shall convey information of the true distance between them. Two examples of covariance matrix distances are the so-called correlation matrix distance (CMD) and the Log-Euclidean (LogEuc) distance. For two covariance matrices $\mathbf{R}_i$ and $\mathbf{R}_j$, they are defined as

$$d_{\mathrm{CMD}}(\mathbf{R}_i, \mathbf{R}_j) = 1 - \frac{\mathrm{Tr}\left(\mathbf{R}_i\mathbf{R}_j\right)}{\|\mathbf{R}_i\|_{\mathrm{F}}\|\mathbf{R}_j\|_{\mathrm{F}}}, \tag{10}$$

$$d_{\mathrm{LogEuc}}(\mathbf{R}_i, \mathbf{R}_j) = \left\|\log(\mathbf{R}_i) - \log(\mathbf{R}_j)\right\|_{\mathrm{F}}. \tag{11}$$

In multi-point CC (MPCC) [15], multiple mMIMO cells collaborate to learn a chart based on CSI at multiple cells. The CSI of each UE is known at multiple but not necessarily all cells. In MPCC, each BS/cell computes a local dissimilarity matrix $\mathbf{D}_c$, for $c = 1, \ldots, C$. A centralized unit then merges the individual dissimilarity matrices into a global matrix

$$\mathbf{D} = \sum_{c=1}^{C} \tilde{\mathbf{F}}_c \odot \mathbf{D}_c, \tag{12}$$

where the (i,j)th element of $\tilde{\mathbf{F}}_c$ is given as

$$\tilde{f}_{c,i,j} = \frac{f_{c,i,j}}{\sum_{c'} f_{c',i,j}}, \text{ with } f_{c,i,j} = \left(\min\{\beta_{c,i}, \beta_{c,j}\}\right)^2.$$

Once the dissimilarity matrix has been constructed, the channel chart is obtained by applying a dimensionality reduction technique on the feature space. One example of such techniques is t-distributed stochastic neighbor embedding (t-SNE), which is based on converting the distances between data points into probabilities related to local neighborhood relations.

There exist many evaluation measures to characterize the quality of channel charts and their ability to preserve the local and global geometry of the true UE locations. Trustworthiness (TW) and continuity (CT) assess the neighborhood preservation quality of the charts, while Kruskal's stress (KS) is a measure of the distance distortion between the space of UE locations and the chart locations.

Assuming that the radio environment is stationary, an OoS algorithm maps new UEs in the network to an existing CC. Finding the CC location for an OoS UE, in the online phase, can be done without the need to repeat the whole CC process.

In MPCC, the chart is constructed by a centralized unit based on a merged dissimilarity matrix. The locations of UEs on the chart are therefore based on merged information from different BSs.

We consider the following approaches to create a MPCC.

- Cell-wise covariance matrix based. Each cell/sector computes its local cell-wise dissimilarity matrix using cell covariance matrix $\mathbf{R}_{c,k}$.
- Sector-selection covariance matrix based. First, the cell-wise dissimilarity matrix is computed using cell covariance matrix $\mathbf{R}_{c,k}$. Then, for each pair of UEs, the dissimilarity of one sector from each BS is selected as in [12].
- BS covariance matrix based. The BS covariance matrices considering all sectors/cells served by the BS are used to compute the dissimilarity matrix. This assumes phase coherence between all sectors in a cell.

The dissimilarity of all cells/BSs is then merged using (12).

To find a MPCC location of an OoS UE in an existing chart, there exist different possibilities. One way would be to redo the merging and then mapping to the chart. This approach cannot be applied if only partial information of the OoS UE is available. In this regard, we adopt a single-point approach; a cell/BS may place the UE on the chart by averaging the chart locations of the k-nearest neighbors (KNN) to the OoS UE based on a covariance matrix dissimilarity.

V. Pilot Allocation

Pilot allocation is the distribution of pilot sequences across UEs. Implementation of a pilot reuse scheme in an intelligent manner promises better spectral efficiency. We will discuss pilot allocation based on a WGC approach.

An undirected weighted graph is defined by $G = (\mathcal{V}, \mathcal{E})$ where $\mathcal{V}$ is the vertex set and $\mathcal{E}$ is the edge set. Each vertex represents a UE, and an edge represents the weight (strength) of the interference between two UEs. The τ-WGC problem aims to assign one colour (i.e., pilot) for each vertex (i.e., UE), given τ pilots, such that the total interference is minimized.

A. Weighted Graph Colouring Problem

The edge set $\mathcal{E}$ of an undirected graph can be represented by a weighting matrix $\mathbf{W}$, such that $w_{i,j} = w_{j,i}$, and $w_{i,i} = 0$, for $i, j = 1, \ldots, K$. We will discuss how the weights are obtained from CSI features, physical locations and chart locations in a following section. The τ-WGC problem can be formulated as:

$$\min_{\mathbf{X}} \operatorname{Tr}\left(\mathbf{X}^{\mathrm{T}}\mathbf{W}\mathbf{X}\right), \tag{13a}$$

$$\text{subject to: } x_{k,\rho} \in \{0, 1\}, \tag{13b}$$

$$\sum_{\rho=1}^{\tau} x_{k,\rho} = 1, \tag{13c}$$

where $k = 1, \ldots, K$, $\rho = 1, \ldots, \tau$, and $\mathbf{X}$ is the pilot allocation matrix, which indicates the pilot assigned to each UE. Each UE is constrained to be allocated exactly one pilot, as (13c). The above problem is a nonlinear integer program, which is NP hard. Finding a valid coloring can be done with a greedy algorithm. Greedy colouring considers the vertices in a specific order, i.e., $v_1, \ldots, v_K$, and assigns to node k the smallest available color not used by $v_1, \ldots, v_{k-1}$ vertices. The degree of vertex i is computed as

$$\varphi_i = \sum_{j=1}^{K} w_{i,j}.$$

We order the vertices based on their degrees, the node of the highest degree is v_1 with $\max_i \varphi_i$. The vertices having higher degree are assigned orthogonal pilots on a priority basis. First τ unique pilots are sequentially assigned to the sorted vertices $v_1, \ldots, v_\tau$ and then, for each subsequent vertex, the pilot with the least cost is assigned to that vertex. The cost of a pilot is calculated by summing of the weights of all vertices assigned the same pilot. This continues until all the vertices are assigned pilots.

B. Benchmark Similarities

A similarity matrix that captures the interference relationship between pairs of UEs is needed. Several large scale channel features and distances are considered for that. We create a similarity matrix for each cell in the network. Then, the network point of view is obtained by averaging the points of view of all cells. In creating the similarity of a cell, it is important to differentiate between a UE served in the cell and another UE that is not served by the cell. The most popular approaches to create the cell similarity matrix are described below.

1) Large scale fading based: The similarity between two UEs at cell c is created using the ratio of large scale fading coefficients, expressed as [16]

$$w_{c,i,j} = \begin{cases} 0 & \text{if } i = j, \\ \left(\frac{\beta_{c,i}}{\beta_{c,j}}\right)^{\alpha} & \text{if } i,\ j \in \mathcal{I}_c, \\ \left(\frac{\beta_{c,j}}{\beta_{c,i}}\right)^{\alpha} & \text{if } i \in \mathcal{I}_c,\ j \notin \mathcal{I}_c, \\ 0 & \text{if } i,\ j \notin \mathcal{I}_c, \end{cases} \tag{14}$$

with $\alpha > 0$ is a tuning parameter.

2) AoA based: The similarity between two UEs at cell c based on their AoAs and large scale fading coefficients is computed as [7]:

$$w_{c,i,j} = \begin{cases} 0 & \text{if } i = j, \\ \left|\frac{\sin\left(\pi r M' \Omega_{c,i,j}\right)}{M' \sin(\pi r \Omega_{c,i,j})}\right|^2 & \text{if } i,\ j \in \mathcal{I}_c, \\ \left(\frac{\beta_{c,j}}{\beta_{c,i}}\right)^{\alpha} \left|\frac{\sin\left(\pi r M' \Omega_{c,i,j}\right)}{M' \sin(\pi r \Omega_{c,i,j})}\right|^2 & \text{if } i \in \mathcal{I}_c,\ j \notin \mathcal{I}_c, \\ 0 & \text{if } i,\ j \notin \mathcal{I}_c, \end{cases} \tag{15}$$

where $\Omega_{c,i,j} = \sin\theta_{c,i} - \sin\theta_{c,j}$.

3) Covariance based: The similarity between two UEs at cell c based on their spatial correlation is computed as [8], [17]:

$$w_{c,i,j} = \begin{cases} 0 & \text{if } i = j, \\ 1 - d_{\mathrm{CMD}}\left(\mathbf{R}_{c,i}, \mathbf{R}_{c,j}\right) & \text{if } i,\ j \in \mathcal{I}_c, \\ \left(\frac{\beta_{c,j}}{\beta_{c,i}}\right)^{\alpha} \left(1 - d_{\mathrm{CMD}}\left(\mathbf{R}_{c,i}, \mathbf{R}_{c,j}\right)\right) & \text{if } i \in \mathcal{I}_c, j \notin \mathcal{I}_c, \\ 0 & \text{if } i,\ j \notin \mathcal{I}_c. \end{cases} \tag{16}$$

The network similarity matrix is obtained by taking the sum of all cell similarity matrices as:

$$\mathbf{W} = \frac{1}{2} \sum_{c} \left(\mathbf{W}_c + \mathbf{W}_c^{\mathrm{T}}\right), \tag{17}$$

where the second term is used to obtain a symmetric matrix.

VI. Learning Framework

Our objective is to avoid estimating the covariance matrix of the UE at several cells and develop a similarity matrix that can be used for pilot allocation with reduced complexity and signaling overhead. The problem addressed here thus is: assuming that the covariance is known only at the serving cell, how can pilots be allocated?

We consider a machine learning framework consisting of an offline and online phase. In the offline phase, the UE channel covariances to multiple BSs/cells are estimated and used to create a MPCC, as discussed in Section IV. In the online phase, the OoS UE covariance to the serving BS/cell is estimated and used to predict the CC location or the covariance matrices at other cells. The CC locations of OoS UEs can then be used to create the graph similarity matrix used to allocate pilots. Figure 1 shows the CC based framework for pilot allocation with partial information.

A. Channel Charting Prediction

The CC created in the offline phase can be leveraged to locate the OoS UEs. After training the network with the CC locations of U users, when a new UE joins the network, its

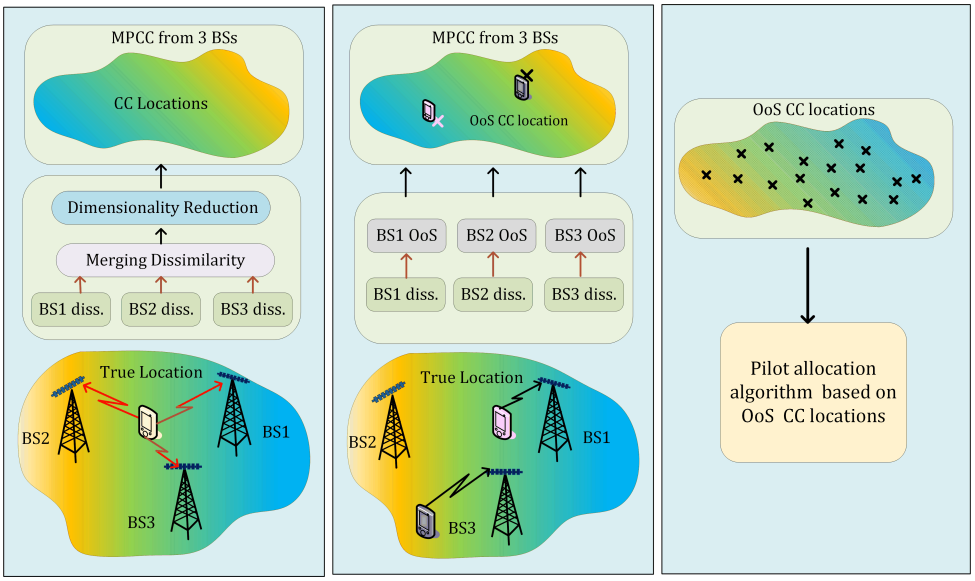

Fig. 1: CC based framework for pilot allocation. (Left): Construction of multi-point CC. (Middle): OoS approach; the covariance matrix is estimated at one BS and the KNN regression is used to find the OoS location. (Right): Pilot allocation based on OoS locations.

CC location can be estimated by averaging the CC locations of its KNN. Hence, the embedding of an OoS UE in the existing CC is done as:

$$\hat{\mathbf{c}}_k = \frac{\sum_{j\in\mathcal{A}_k} \mathbf{c}_j}{|\mathcal{A}_k|}, \tag{18}$$

where $\mathcal{A}_k$ is the KNN set of UE k based on feature distance and $\{\mathbf{c}_j\}$ are the CC locations of the KNN. Herein, we consider a weighted graph obtained by pairwise CC locations, given as

$$w_{c,i,j} = \begin{cases} 0 & \text{if } i = j, \\ \exp\left(-\frac{\|\mathbf{c}_i - \mathbf{c}_j\|_2}{a}\right) & \text{if } i,\ j \in \mathcal{I}_c, \\ \left(\frac{\beta_{c,j}}{\beta_{c,i}}\right)^{\alpha} \exp\left(-\frac{\|\mathbf{c}_i - \mathbf{c}_j\|_2}{a}\right) & \text{if } i \in \mathcal{I}_c,\ j \notin \mathcal{I}_c, \\ 0 & \text{if } i,\ j \notin \mathcal{I}_c. \end{cases} \tag{19}$$

where a is a scaling parameter which is heuristically chosen to normalize the CC distance.

B. Covariance Prediction

The covariance matrices collected in the offline phase can be leveraged to predict the covariance matrix of an OoS UE at other cells in the online phase. Hence, the predicted covariance of UE k on cell c' is computed as

$$\hat{\mathbf{R}}_{c',k} = \frac{\sum_{j\in\mathcal{A}_k} \mathbf{R}_{c',j}}{|\mathcal{A}_k|}, \tag{20}$$

where $\{\mathbf{R}_{c',j}\}$ are the covariance matrices of the KNN at cell c'. The weight similarity then can be computed using (16).

C. Computational Complexity and Communication Overhead

We focus on the computational complexity and communication overhead of the online phase for both CC and covariance prediction. Finding the KNN sets of OoS UEs has the same complexity in both approaches, as it bases on a covariance matrix distance, e.g., Log-Euclidean. After the KNN are found, in the case of CC prediction, the location for each OoS UE is found as (18). In the case of covariance prediction, a cell finds it as (20). Moreover, all cells/BSs, except the serving one for each UE, predict the covariance matrices of all OoS UEs, after receiving their KNN sets. For CC prediction, a centralized unit, after receiving the CC locations from all cells, computes the weight matrix as (19). In the case of covariance prediction, each cell/BS computes its weight matrix as (16). All cells send their matrices to a centralized unit, which then forms a centralized matrix.

For the CC approach, computations only involve 2D vectors, and only the predicted CC locations of OoS UEs are sent to the centralized unit. In the covariance approach, computations involve larger matrices. Moreover, the information exchange is significantly higher. First, the KNN sets of all OoS UEs are required at all cells. In addition, each cell sends a $K \times K$ weight matrix to the centralized unit. Thus, the computational complexity and communication overhead of the online phase is much lower with CC than with covariance prediction.

VII. Simulation Results

We consider a mMIMO system consisting of $B = 7$ BSs, each with $S = 3$ sectors. The simulation parameters are summarized in Table I. Simulation is carried out in two phases. In the offline phase, we consider $U = 4000$ UEs uniformly distributed across the network. We assume a cell can estimate the channel covariance of a UE if the received SNR is greater than some threshold (e.g., -20 dB).

We consider the three different methods discussed in Section IVfor merging the information of sectors served by a BS

TABLE I: Simulation parameters.

Parameter	Value
Num. of BSs B	7
Num. of sectors S	3
Num. of ant. M'	32
Inter-site distance	500 m
Carrier frequency f_c	2 GHz
Bandwidth	50 MHz
BS height	25 m
Norm. ant. spa. μ	0.5
$L_{b,k}$[dB]	$166.44 - 20\log_{10} f_c - 39.08\log_{10} d_{b,k}$
Ang. dev. σ_ϕ	10°
Num. of UEs	4000 (offline), 1000 (online)
UE height	1.5 m
$G_{\max}$, $A_{\max}$	0 dB, 30 dB
Num. of pilots τ	$[10,\ 80]$
Noise power σ_n^2	-90 dBm
Signal power	23 dBm

TABLE II: CC performance, neighborhood of 50 points is used to compute TW and CT.

MPCC approach	TW↑	CT↑	KS↓
Sector merging	0.94	0.95	0.36
Sector merging as in [12]	0.89	0.96	0.47
BS merging, covariance full	0.99	0.99	0.15

to a MPCC. After getting the merged dissimilarity matrix, we apply t-SNE to obtain the MPCC. Simulation results show that the Log-Euclidean distance provides better CCs than the correlation matrix distance. Based on this, we report CC results with Log-Euclidean distance. The CC performance for the above discussed approaches are summarized in Table II. The CC of BS covariance matrix based approach is much better than the sector based. We will use this chart for pilot allocation below.

In the online phase, we consider $K = 1000$ UEs, the channel covariance matrix for each UE is estimated only at the cell/ BS with the largest SNR. The dissimilarity of an OoS UE is computed with respect to the offline UEs in the same cell/BS, i.e., UEs with SNR above the given threshold. This dissimilarity vector is used to find the KNN and predict the CC of OoS UE using (18), where $k = 1$ is selected. To find the

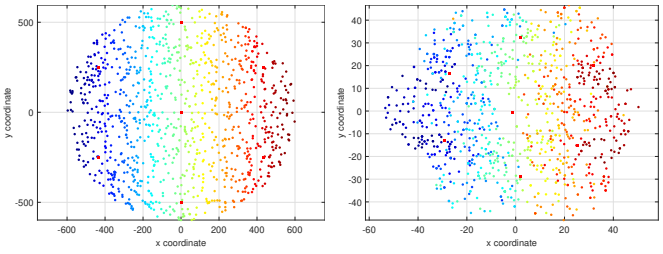

Fig. 2: (Left): Physical Locations of UEs. (Right): Channel chart for OoS UEs. CC locations are marked by colours corresponding to the physical locations in (Left).

OoS CC location we consider both the covariance at the serving cell, and the full covariance at the serving BS. Figure 2 shows the CC of the OoS users based on the covariance at the BS and their corresponding physical locations. The performance measures of the CC are obtained as TW$= 0.94$ and CT$= 0.93$, considering 50 neighbours, and KS$= 0.24$.

To benchmark the performance of the CC based pilot allocation, we consider the following approaches to obtain a weighted matrix on which greedy pilot allocation is done:

- Large scale fading based: The similarity is computed as in (14).
- AoA based: The similarity is computed as in (15).
- Covariance matrix based with full information: The similarity is computed as is computed as in (16).
- Covariance matrix based with partial information: The similarity is computed as in (16). However, the similarity is computed only between UEs in the same cell.
- Pair-wise physical distance based: The similarity is computed by replacing the CC distance in (19) with true physical distance. This approach is not discussed in the literature.

In each similarity matrix, α is experimentally tuned to get the best performance. For CC-based method, we have chosen $\alpha = 0.5$.

In addition, we consider a machine learning approach to predict the channel covariance matrices of the OoS UEs at other cells based on (20). Then we obtain the similarity based on predicted covariance matrices using (16), and apply the greedy pilot allocation algorithm. Furthermore, we consider random pilot allocation.

The performance of each algorithm is evaluated in terms of the NMSE, given by (9). Figure 3 shows the NMSE as a function of pilot length τ for the CC based approach compared to the benchmark schemes. As expected, when increasing the length of the orthogonal pilot sequences, the number of interfering UEs per pilot sequence decreases and thus, NMSE improves. Pilot allocation based on covariance matrix with full information shows the best performance, while the covariance matrix based with partial information results in degraded performance due to the lack of coordination between cells. The NMSE performance of AoA based approach is worse than the covariance matrix based with full information, this is because the AoA similarity weight is suitable for line-of-sight scenarios and not suitable for non-line-of-sight scenarios. The performance of CC based is indistinguishable from pair-wise physical distance scheme. The NMSE performance of the predicted covariance based approach is close to the performance of covariance matrix based with full information. The NMSE performance of CC prediction based on the covariance of only the serving cell is a little degraded compared CC prediction based on the covariance of the serving BS. In the latter case, the prediction is based on knowing more information about the UE. The random pilot allocation has the worst NMSE performance.

Figure 4 shows the NMSE as a function of SNR for $\tau = 40$. We consider the SNR of a reference UE at a distance of

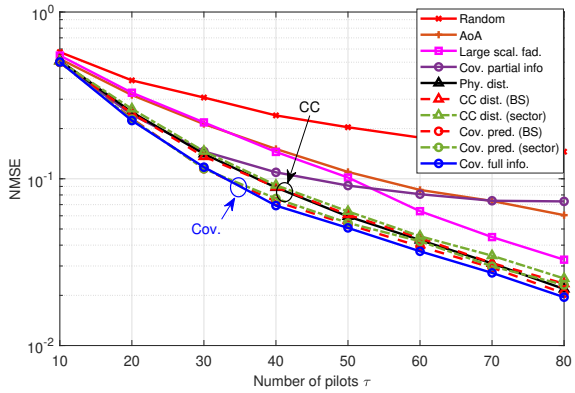

Fig. 3: NMSE performance of CC based approach compared to different approaches as a function of the number of pilots.

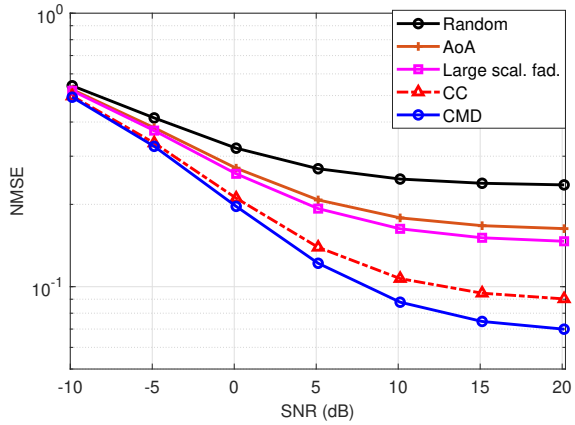

Fig. 4: NMSE performance of different approaches as a function of SNR for $\tau = 40$.

100 m from its serving BS. We consider pilot allocation based on random, AoA, large scale fading, covariance with full information and CC. The figure shows that CC based approach has good performance at all SNR values. At low SNR values, it approaches the performance of the covariance based scheme with full information.

VIII. Conclusions

In this paper, we developed a pilot allocation framework based on channel charting (CC) in a multi-cell network with spatially correlated MIMO channels. The CC is constructed in an offline phase, where UE covariance matrices at multiple BSs are estimated. In the online phase, partial information about UE channel covariance matrix is assumed, i.e., the UE channel covariance is known only by the serving BS. We considered k-nearest neighbor approach to locate the out-of-sample UEs on the CC. The multi-point CC provides a global network view of the geometry. In this regard, we have utilized the CC distances to create the weight similarity matrix, which is then used to allocate the pilots based on a greedy algorithm. We compare the performance of the CC based scheme with other approaches from the literature using normalized mean squared error. The performance of the CC based pilot allocation outperforms the one based on AoA from the literature and approaches the performance of the covariance matrix based solution with full information. The performance of the CC based pilot allocation is indistinguishable from the one based on physical location, verifying that CC locations can be used as proxies for physical locations in RRM tasks. The proposed framework will be verified using measured channels in future work.

Acknowledgements

This work was funded in part by the Research Council of Finland (RCF) grant 345109, by CHIST-ERA project CHASER (CHIST-ERA-22-WAI-01) through RCF grant 359837, the RCF via 6G Flagship grant 318927, and the Higher Education Commission of Pakistan.

References

[1] T. L. Marzetta, "Noncooperative cellular wireless with unlimited numbers of base station antennas," *IEEE Trans. Wireless Commun.*, vol. 9, no. 11, pp. 3590–3600, 2010.

[2] O. Elijah, C. Y. Leow, T. A. Rahman, S. Nunoo, and S. Z. Iliya, "A comprehensive survey of pilot contamination in massive MIMO—5G system," *IEEE Commun. Surveys Tuts.*, vol. 18, no. 2, pp. 905–923, 2016.

[3] H. Yin, D. Gesbert, M. Filippou, and Y. Liu, "A coordinated approach to channel estimation in large-scale multiple-antenna systems," *IEEE J. Sel. Areas Commun.*, vol. 31, no. 2, pp. 264–273, 2013.

[4] H. Echigo, T. Ohtsuki, W. Jiang, and Y. Takatori, "Fair pilot assignment based on AoA and pathloss with location information in massive MIMO," in *Proc. IEEE Globecom*, 2017, pp. 1–6.

[5] A. S. Al-Hubaishi, N. K. Noordin, A. Sali, S. Subramaniam, and A. M. Mansoor, "An efficient pilot assignment scheme for addressing pilot contamination in multicell massive MIMO systems," *Electronics*, vol. 8, no. 4, 2019.

[6] L. S. Muppirisetty, T. Charalambous, J. Karout, G. Fodor, and H. Wymeersch, "Location-aided pilot contamination avoidance for massive MIMO systems," *IEEE Trans. Wireless Commun.*, vol. 17, no. 4, pp. 2662–2674, 2018.

[7] N. Akbar, S. Yan, N. Yang, and J. Yuan, "Location-aware pilot allocation in multicell multiuser massive MIMO networks," *IEEE Trans. Veh. Technol.*, vol. 67, no. 8, pp. 7774–7778, 2018.

[8] L. You, X. Gao, X.-G. Xia, N. Ma, and Y. Peng, "Pilot reuse for massive MIMO transmission over spatially correlated Rayleigh fading channels," *IEEE Trans. Wireless Commun.*, vol. 14, pp. 3352–3366, 2015.

[9] C. Studer, S. Medjkouh, E. Gonultaş, T. Goldstein, and O. Tirkkonen, "Channel Charting: Locating users within the radio environment using channel state information," *IEEE Access*, vol. 6, pp. 47 682–47 698, 2018.

[10] P. Kazemi, H. Al-Tous, T. Ponnada, C. Studer, and O. Tirkkonen, "Beam SNR prediction using channel charting," *IEEE Trans. Veh. Technol.*, vol. 72, no. 10, pp. 13 130–13 145, 2023.

[11] L. Ribeiro, M. Leinonen, H. Al-Tous, O. Tirkkonen, and M. Juntti, "Channel charting aided pilot reuse for massive MIMO systems with spatially correlated channels," *IEEE Open J. Commun. Soc.*, vol. 3, pp. 2390–2406, 2022.

[12] L. Ribeiro, M. Leinonen, I. Rathnayaka, H. Al-Tous, and M. Juntti, "Channel charting aided pilot allocation in multi-cell massive MIMO mMTC networks," in *Proc. IEEE SPAWC*, 2022, pp. 1–5.

[13] D. G. Riviello, F. D. Stasio, and R. Tuninato, "Performance analysis of multi-user MIMO schemes under realistic 3GPP 3-D channel model for 5G mmWave cellular networks," *Electronics*, vol. 11, no. 3, 2022.

[14] E. Björnson, J. Hoydis, and L. Sanguinetti, *Massive MIMO Networks: Spectral, Energy, and Hardware Efficiency*. Hanover, MA, USA: Now Publishers Inc., 2018.

[15] J. Deng, S. Medjkouh, N. Malm, O. Tirkkonen, and C. Studer, "Multi-point channel charting for wireless networks," in *Proc. Asilomar Conf. Sign., Syst., Comput.*, Oct. 2018, pp. 286–290.

[16] X. Zhu, L. Dai, Z. Wang, and X. Wang, "Weighted-graph-coloring-based pilot decontamination for multicell massive MIMO systems," *IEEE Trans. Veh. Technol.*, vol. 66, no. 3, pp. 2829–2834, 2017.

[17] W. Zhong, L. You, T. Lian, and X. Gao, "Multi-cell massive MIMO transmission with coordinated pilot reuse," *Science China Technological Sciences*, vol. 58, pp. 2186–2194, Nov. 2015.